# Supporting Information

## Be'er et al. 10.1073/pnas.1001062107

### SI Text

**Model** We present a model describing the dynamics of some major constituents of the bacterial colony. The purpose of the model is to understand how the bacteria, nutrients, and subtilisin combine to give the observed behavior of the colonies. In the model, at the front of a single growing colony, the prespore and subtilisin concentrations reach steady state constant values. With two colonies competing for resources, this steady state cannot be maintained, resulting in an increase in subtilisin concentration. This then triggers production of the sibling lethal factor (Slf) protein, stopping the growth of neighboring colonies toward one another.

Previous approaches for modeling bacterial colonies can be categorized as either continuous models involving coupled reaction–diffusion equations or discrete agent-based models with a moving interface (see 1 for a review). Continuous models describe the coarse-grained density of bacteria and other system constituents as continuous fields whose dynamics is given by a system of partial differential equations. With nonlinear diffusion for the bacteria, the system admits solutions with a compact support (2). This is in accord with the experimental observation that the bacteria swim in a lubrication layer (1, 3) that has a well-defined edge. On the other hand, agent-based simulations are useful for describing the internal mechanism of each agent (in our case a group of bacteria) and their mutual interactions. The time evolution of the colony can be described by a dynamic boundary. The interaction between the agents and the boundary is specified via appropriate boundary conditions and a dynamic equation for the moving interface.

In our model the concentrations of bacteria $b(t)$, nutrients $n(t)$, prespores $p(t)$, subtilisin $s(t)$, and Slf $x(t)$ are continuous fields, and the outer effective envelope of the colony is given by a smooth impenetrable time-dependent curve $\gamma(t)$ (which is within the domain). This approach differs from models in which the bacterial density continuously decreases to zero at the edge of a colony (1, 2, 4), but our model is in accord with the observations that the concentration of bacteria is high near the edge of the colony and drops abruptly to zero, as illustrated in Fig. S6 (from ref. 5), where the bacteria are active only in a region about 0.3 mm wide in a colony of diameter 40 mm. Live bacteria exist further inside a colony, but they are considerably less active and do not seem to influence the propagation speed of the interface (3, 5). We are interested in describing the coarse-grained behavior of the colony rather than the exact shape of the edge of the lubrication layer. As such, we do not attempt to model the complicated fingering patterns seen, for example, in Fig. 1. Accordingly, the contribution of surface tension and surface active materials is treated phenomenologically through an effective formula that describes how the dynamics of the interface depends on the local fields.

Because the bacteria swim in a liquid that is extracted from the agar gel, moving the envelope requires additional liquid. We assume that each bacterium can extract or produce liquid at a rate that depends on available food. Hence, the envelope moves with a normal speed that increases with nutrient concentration and is proportional to the bacterial concentration close to the edge of the envelope. The velocity of the front at time $t$ takes the form

$$\dot{\gamma}_n = \text{front speed}(b,n), \qquad \textbf{[S1]}$$

where the dot represents differentiation with respect to time; $\dot{\gamma}_n$ denotes the speed of a point on the interface curve in a direction normal to the curve. The fields $b$ and $n$ themselves depend on the solution in the entire domain.

The diffusion–reaction part of the model is as follows. Inside the envelope bacteria move by diffusion and chemotaxis, but cannot cross the boundary $\gamma(t)$. In other words, the bacterial flux, which is later defined in Eq. **S3**, vanishes across the envelope. Bacteria reproduce, consume food, become prespores at low food concentrations, and die from Slf (thus Slf removes bacteria from the system). Prespores become spores or die from Slf. Food diffuses and is consumed by the bacteria and prespores. Subtilisin, assumed to be produced by prespores, diffuses and degrades. Slf, produced by bacteria in stress (at high bacterial and subtilisin concentrations), diffuses and degrades as well. Schematically, the model is given by the following coupled equations:

$$\begin{cases} \dot{b} = \text{movement}(b,n) + \text{reproduction}(b,n,s,x) \\ \qquad - \text{presporulation}(b,n) - \text{death}(b,x) \\ \dot{p} = \text{presporulation}(b,n) - \text{sporulation}(p) - \text{death}(p,x) \\ \dot{n} = \text{diffusion}(n) - \text{consumption}(b,p,n) \\ \dot{s} = \text{diffusion}(s) + \text{production}(p) - \text{degradation}(s) \\ \dot{x} = \text{diffusion}(x) + \text{production}(b,s,x) - \text{degradation}(b,p,x). \end{cases} \qquad \textbf{[S2]}$$

The above equation for $b$ only holds inside the colony; outside the colony the bacterial density is always zero. Experiments suggest that both subtilisin and Slf become inactive when in contact with the Petri dish wall (3). Boundary conditions are chosen accordingly:

- bacteria: At the edge of the colony the velocity of bacteria in the direction normal to the front cannot exceed that of the front itself. Hence, there is no bacterial flux across the envelope $\gamma$. The bacterial flux, $J_b$, is defined later in Eq. **S3**.
- prespores: No boundary data.
- nutrient: No-flux across a large disk marking the edge of the Petri dish.
- subtilisin: Vanishes on a large disk marking the edge of the Petri dish.
- Slf: Vanishes on a large disk marking the edge of the Petri dish.

In simulations that involve two colonies that are symmetric across the median line of the dish, we solve the equations in only half the domain; boundary conditions for $s$ and $x$ across that axis are no-flux. The computational domain and the boundary conditions for simulations in the case of two colonies are depicted in Fig. S7.

The functional form for the schematic expressions above as used in our simulations is as follows, where $H(z)$ denotes the Heavyside function, $H(z) = 1$ if $z \geq 0$ and zero otherwise. Unless specified otherwise, all other symbols are positive constants.

- bacteria, $b$:

$$\begin{aligned} &\text{movement}(b,n) = D_b \nabla \cdot J_b \\ &J_b = \nabla b - \frac{k_c}{(1+n/k_{c0})^2} b \nabla n \\ &\text{furthermore, } b \text{cannot exceed} b_{\max}. \\ &\text{reproduction}(b,n,s,x) = \min\{1,n\} b(1-b/b_{\max}) \\ &\quad \times (\mu_0 + \mu_s s) H(x_c - x) \\ &\text{presporulation}(b,n) = \mu_{ps} b e^{-a_{ps} n} \\ &\text{death}(b,x) = \mu_x b(e^x - 1). \end{aligned} \qquad \textbf{[S3]}$$

The first term in the bacterial flux $J_b$ describes the diffusion of bacteria. The second term describes chemotaxis toward high food concentrations (2). At low nutrient concentrations, reproduction is proportional to food availability. In addition, reproduction saturates at $b_{\max}$, increases linearly with $s$, and stops if $x > x_c$. Note that with $n \geq 1$ and $s = 0$, the reproduction rate is proportional to the parameter $\mu_0$. The rate of presporulation decreases exponentially with food. Bacterial death from Slf increases exponentially with $x$.

- prespores, $p$:

$$\text{sporulation}(p) = \mu_s p \qquad \text{death}(p,x) = \mu_{px} p(e^x - 1). \qquad \textbf{[S4]}$$

Prespores become spores at a constant rate and die from Slf at a rate that increases exponentially with $x$.

- nutrient, $n$:

$$\begin{aligned} \text{diffusion}(n) &= D_n \nabla^2 n \\ \text{consumption}(b,n) &= \min\{1,n\}(\lambda_b b + \lambda_p p). \end{aligned} \qquad \textbf{[S5]}$$

Nutrients are consumed by bacteria and prespores. Further, at low food concentration, consumption is reduced because not all bacteria can get all the food they require.

- subtilisin, $s$:

$$\begin{aligned} \text{diffusion}(s) &= D_s \nabla^2 s \\ \text{production}(p) &= \nu_s p \\ \text{degradation}(s) &= \nu_s s. \end{aligned} \qquad \textbf{[S6]}$$

Subtilisin is produced at a constant rate by prespores and degenerates at a constant rate.

- Slf, $x$:

$$\begin{aligned} \text{diffusion}(x) &= D_x \nabla^2 x \\ \text{production}(b,s,x) &= \nu_x b H(s - s_c) H(b - b_c) \\ \text{degradation}(b,p,x) &= x(\nu_{dx} + \nu_{db} b + \nu_{dp} p). \end{aligned} \qquad \textbf{[S7]}$$

At high bacterial concentrations, $b > b_c$, and at high subtilisin concentrations, $s > s_c$, bacteria produce Slf at a rate proportional to $b$. Degradation occurs either spontaneously or by contact with bacteria and prespores.

- envelope:

$$\text{front speed}(b,n) = v_{\max} \frac{b}{b_{\max}} (1 - e^{-a_f n}). \qquad \textbf{[S8]}$$

The front moves at a speed that is proportional to the local bacterial concentration and increases nonlinearly with food to a maximal speed $v_{\max}$. The exact functional dependence of the front's speed on $n$ has no qualitative impact on the results. We use an exponential dependency that is smooth and has favorable analytical and numerical properties.

*Remark:* The internal limit of the flux term for $b$, $J_b$ in Eq. **S3**, does not necessarily vanish at the edge of the colony due to the chemotactic term that involves $\nabla n$. This is in accord with our observation that the concentration of bacteria is highest near the edge of the colony and that bacteria are attempting to get closer to regions with more food. However, the bacterial motion does not seem to be the source of the boundary's motion (5). In simulations, the conservation law for $b$ is maintained on the inside of $\gamma$ by canceling all bacterial flux terms that enter or leave the colony; hence the bacteria cannot penetrate the interface. In addition, flux terms may be decreased to force the maximal concentration condition.

**Results** One of the main predictions of the model is that the concentration of subtilisin at the front of a single growing colony, where most of the motile bacteria are located, is maintained at some fixed value (see text and Fig. 4*A*). Disruption of this steady state affects the colony dynamics, as observed both with two colonies and in the experiments with added subtilisin.

For a single colony, the growth of the colony is limited by the flux of food through the envelope. After an initial lag time during which the bacteria do not move, the system reaches a state in which the concentrations of bacteria, subtilisin, and nutrient close to the envelope are practically constant. As a result, the envelope advances with constant velocity.

With an external source of subtilisin, the steady state cannot be maintained, and the bacteria face two contradictory signals. On one hand, with enough food, bacterial density may be high, close to maximum. On the other hand, the subtilisin concentration is high, indicating a high concentration of prespores and hence low bacterial density. The conflict cannot be resolved through sporulation, as prespores produce even more subtilisin. The solution of the dilemma is to trigger production of a new protein, Slf, which quickly reduces the bacterial population until more favorable conditions occur.

With two colonies in the early stages of growth, the colonies do not sense one another, and they each grow independently with a constant velocity of the envelope. However, as the two colonies approach, the depletion of nutrients leads to a slowing of the growth. At a later stage, the extra subtilisin coming from the neighboring colony and the increased presporulation rate disrupts the subtilisin steady state. This triggers production of the Slf protein, bringing the growth of the colonies to a halt.

***Numerical Implementation.*** Methods for simulating dynamical interfaces can be generally divided into three categories: interface tracking methods (6), phase-field methods (7, 8) and level-set methods (9). The simulations leading to Fig. 4 involve a two-dimensional smooth interface whose dynamics does not undergo any topological changes (i.e., merging or splitting of curves). Hence, all three approaches can be applied to our model successfully. In this paper the model was solved numerically using a level-set function to describe the envelope (9). This approach provides a simple and natural formalism for describing the dynamics of the moving interface. In particular, the level-set method (9) provides a convenient setting for implementing the bacterial no-flux boundary condition across the interface.

Let $D$ denote a $L_x \times L_y$ rectangle on the plane. Let $\gamma(t)$ denote the set of points that forms the envelope curve at time $t \geq 0$, i.e., a point $(x,y)$ in $D$ is in $\gamma(t)$, $(x,y) \in \gamma(t)$, if and only if $(x,y)$ is a point on the envelope at time $t$. We assume that the curve $\gamma(t)$ is smooth. Let $v_n(t,x,y)$ denote the speed of a point $(x,y) \in \gamma(t)$ in the normal direction. In our model, $v_n = \text{front speed}(b,n)$. Let $\varphi(t,x,y)$ denote a function on $[0,T] \times D$ such that

1. $\varphi$ is smooth.
2. at time $t = 0$, $\varphi$ is negative inside $\gamma(0)$ (inside the colony) and positive outside $\gamma(0)$.
3. $\varphi$ satisfies the partial differential equation

$$\frac{\partial \varphi}{\partial t} + v_n |\nabla \varphi| = 0. \qquad \textbf{[S9]}$$

Then, it can be shown (6) that, for all $t \geq 0$, we have that $\{(x,y) | \varphi(t,x,y) = 0\} = \gamma(t)$. In other words, the zero level-set of $\varphi$ at time $t$ is exactly the envelope at time $t$, $\gamma(t)$ and the front moves with the correct normal speed $v_n$. Furthermore, the function is always negative inside $\gamma$ and positive outside.

In principle, the expression for $v_n$, Eq. **S8**, is only defined inside the colony where the bacteria are located. Accordingly, we extend

$v_n$ to the outside of the colony in a self consistent and continuous manner. For simplicity, we take $v_n$ to be constant in the direction perpendicular to $\gamma$. This is done by solving the following auxiliary equation for $v_n$ in the domain $\varphi > 0$ (9):

$$\frac{\partial v_n}{\partial t} + K\nabla v_n \cdot \nabla\varphi = 0, \qquad \textbf{[S10]}$$

for some large constant $K > 1$. Indeed, we notice that at equilibrium, the solution of Eq. **S10** satisfies $\partial v_n/\partial t = 0$ and hence $\nabla v_n \cdot \nabla\varphi = 0$. Because $\gamma$ is a level-set of $\varphi$, $v_n$ is constant in the direction perpendicular to it. Outside the Petri dish the $v_n$ satisfies

$$\frac{\partial v_n}{\partial t} + K\nabla v_n \cdot r = 0, \qquad \textbf{[S11]}$$

where $r$ is a unit vector pointing away from the dish center. As before, at equilibrium we have that $\nabla v_n \cdot r = 0$. The no-flux condition for $n$ is maintained in a similar way. Hence, we obtain a no-flux condition outside the dish. In addition, we pick an initial $\varphi$ such that $|\nabla\varphi| = 1$ except at a few vertices. We also perform auxiliary smoothing steps to insure $\varphi$ is smooth and that $|\nabla\varphi| = 1$, as suggested in (6). However, because the boundary is only moving forward, we only smooth the outside of the colony. In addition, as $\varphi$ is changed and the colony claims new territory, initial conditions at new positions are $b = 0$, and hence $v_n = 0$. These positions are gradually filled by the moving bacteria. Note that $v_n$ is nonnegative and the boundary only moves forward. Therefore, the opposite situation in which the bacteria lose ground does not happen. The set of Eqs. **S2–S11** are solved on a rectangular grid.

Finally, we comment on numerical discretization of derivatives. Diffusion and other movement terms for bacteria are discretized in a conservative way to make sure that quantities are conserved at the numerical level. In particular, fluxes are calculated at midpoints (10). Let $z_{i,j}$ denote the value of field $z$ at the $(i,j)$ grid point, $z = b, p, n, s$ or $x$. Also, let $z_{i\pm1/2,j} = (z_{i,j} + z_{i\pm1,j})/2$, and similarly for $z_{ij\pm1/2}$. Then, for example, the bacterial movement term described in Eq. **S2** is calculated as the sum of four flux terms:

$$\text{movement}(b,n) = D_b(\text{left} + \text{right} + \text{up} + \text{down}),$$

where left, right, up, and down denote the bacterial flux from the corresponding directions. To implement Eq. **S2** with a method that conserves $b$, we take

$$(\Delta x)^2\text{left} = \frac{1}{2}(b_{i-1,j} - b_{i,j}) + b_{i-1/2,j}\frac{k_c}{(1 + n_{i-1/2,j}/k_{c0})^2}b_{i-1/2,j}(n_{i,j} - n_{i-1,j}),$$

where $\Delta x$ denotes the grid spacing in the $x$ direction. Flux terms from other directions are discretized in a similar way. As explained above, bacterial flux terms that exit or enter the colony are canceled. In addition, flux terms may be decreased to force the maximal concentration condition, $b \le b_{\max}$. The conservation law for $b$ was verified numerically in a simulation with no reproduction, presporulation, and death terms.

The only physical meaning for $\varphi$ is its zero level-set; hence information for evolving $\varphi$ should depend on that region. Therefore, spatial derivatives for $\varphi$ are calculated using a first order upward scheme. Because $v_n > 0$, the characteristics of Eq. **S9** are pointing away from $\varphi = 0$. Accordingly, the direction of derivatives is $\nabla\varphi$ outside the colony and $-\nabla\varphi$ inside. Spatial derivatives for the extended $v_n$ outside the colony are also taken as upwind in the direction of $\nabla\varphi$ or $r$, outside the colony or outside the dish, respectively. Gradients appearing in $J_b$ are also calculated using an upwind scheme so that close to the boundary, derivatives are taken from the inside of the colony. Laplacians are discretized using central difference, and time stepping is done using forward Euler.

***Simulation Details for Fig. 4*** Fig. 4 shows simulation results for two neighboring colonies. As explained above, we take advantage of symmetry and only simulate half a dish with a single colony. To reproduce conditions that are similar to experiments, the initial colony has a radius of 0.25 and is centered at (0.85, 4.4). The two colony case is described by the left side of the simulated colony, whereas the single colony case is described by the right side, which is independent of the other colony. Because units in simulations are arbitrary, some variables (including time) appearing in Fig. 4 were rescaled. Other simulation parameters are given in Table S1.

**Edman Sequencing of Flagellin and Subtilisin.** ***Amino Acid Sequencing of Flagellin.*** The sequence matched the predicted protein for an open reading frame (ORF) of size 28.980 kDa in the *paenibacillus dendritiformis* genome. The sequence of the predicted protein is:

**MSMFINTNVGAINAHRNLGMNN**TAMGKTMEKLSSGFRINRAADDAAGLAISEKMRFQIGGMNQAMRNAQDGISLIQTAEGALTEVHSMLQRLNTLANQSATGTYDEKDRENTQKEVDALLAEIDNIASSTKFNGIELLSKTGKVSFQIGVTKDNVLTADLAKMDTNALKLNGLSIGTQTNASSALAKIEAAINQVSEQRASFGAVQNRLEHTINNLGVTAENLSASESRIRNADMAKEMTDFTRNQILVQAGTAMLAQANSAPQSVLKLLG

Bold indicates the peptide sequence determined for the isolated protein.

***Amino Acid Sequencing of Subtilisin.*** The sequence matched the predicted protein for an open reading frame (ORF) of size 60.245 kDa in the *paenibacillus dendritiformis* genome. The sequence of the predicted protein is:

MKKFLSSVLAAILLMVTLLTGVSFGSPAEGHSSDYIEGQLVVSLEEPFMDSSQSVDDILMEADSLTESGFAIADSLFGQDAGTFSVQALDSDVRATAIEKMGLVYLVEYSVKDYKSIESAKNTLEKKLDNLGFHVRYISENRKMYALETATVQDVSPQ**AIHNNQRWHYEMIKVPQAW**EITAGSSSVRIGVLDTGIDSNHPSLKDLVNTSLGSSFVGGTTNDGNGHGTHVAGTIASYGSVSGVMQNATLIPIKVLNDSGSGSLYGVQQGIVYAANIRADVINMSLGGGGYDQGMDEAIQTAVSLGTIVVAAAGNDGRPSISYPAAYSGSIAVGSVTSSRTRSSFSNYGPGLDVMAPGSNIYSTYKNGQYTTLSGTSMATPHVTGVFGLMRSVNPNLSPAAAGDILRNTAQPAGSSDQYGHGIVDAHAAVLAAAGGGDTPAPSAPGDLISTGQTGTSVSLSWNPPTDNEGVTAYEVYNGDSLAATVANTSATVTDLTADTTYTFTVRAVDASGNRSEASNAVTVTTDSDSSQPSPTWAPGISYKIGEEVTYGEATYQCLQEHISMAGWEPLNVPALWLEK

Bold indicates the peptide sequence determined for the isolated protein.


1. Ben-Jacob E, Cohen I, Levine H (2000) Cooperative self-organization of microorganism. *Adv Phys* 49:395–554.
2. Kozlovsky Y, Cohen I, Golding I, Ben-Jacob E (1999) Lubricating bacteria model for branching growth of bacterial colonies. *Phys Rev E* 59:7025–7035.
3. Be'er A, et al. (2009) Deadly competition between sibling bacterial colonies. *Proc Natl Acad Sci USA* 106:428–433.
4. Dahmen KA, Nelson DR, Shnerb NM (1999) Population dynamics and non-Hermitian localization: Statistical mechanics of biocomplexity. *Lect Notes Phys* 572:124–151.
5. Be'er A, et al. (2009) Paenibacillus dendritiformis bacterial colony growth depends on surfactant but not on bacterial motion. *J Bacteriol* 191:5758–5764.
6. Tornberg AK, Engquist B (2003) The segment projection method for interface tracking. *Comm Pure Appl Math* 56:47–79.
7. Karma A, Kessler DA, Levine H (2001) Phase-field model of mode III dynamic fracture. *Phys Rev Lett* 87:45501.
8. Karma A, Rappel W-J (1996) Numerical simulation of three-dimensional dendritic growth. *Phys Rev Lett* 77:4050–4053.
9. Osher S, Fedkiw RF (2003) Level Set Methods and Dynamic Implicit Surfaces: Applied Mathematical Sciences (Springer–Verlag, New York), pp 153.
10. Leveque RJ (1992) Numerical methods for conservation laws. (Birkhauser–Verlag, Basel).

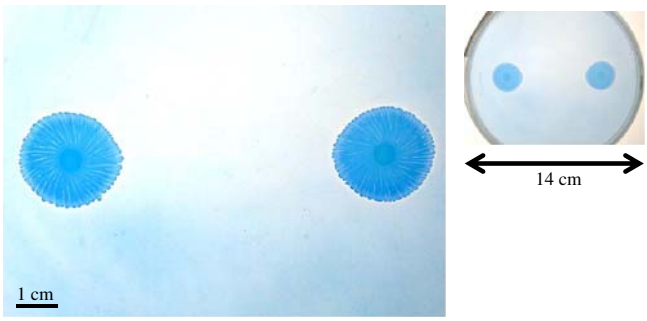


**Fig. S1.** Early stage of interaction between neighboring *P. dendritiformis* colonies that are separated by 7 cm, which is much further than the initial separation of the inoculants in the experiments in the text (1.2 cm). Here, after 4.5 d of growth, the colonies show a weak attraction.

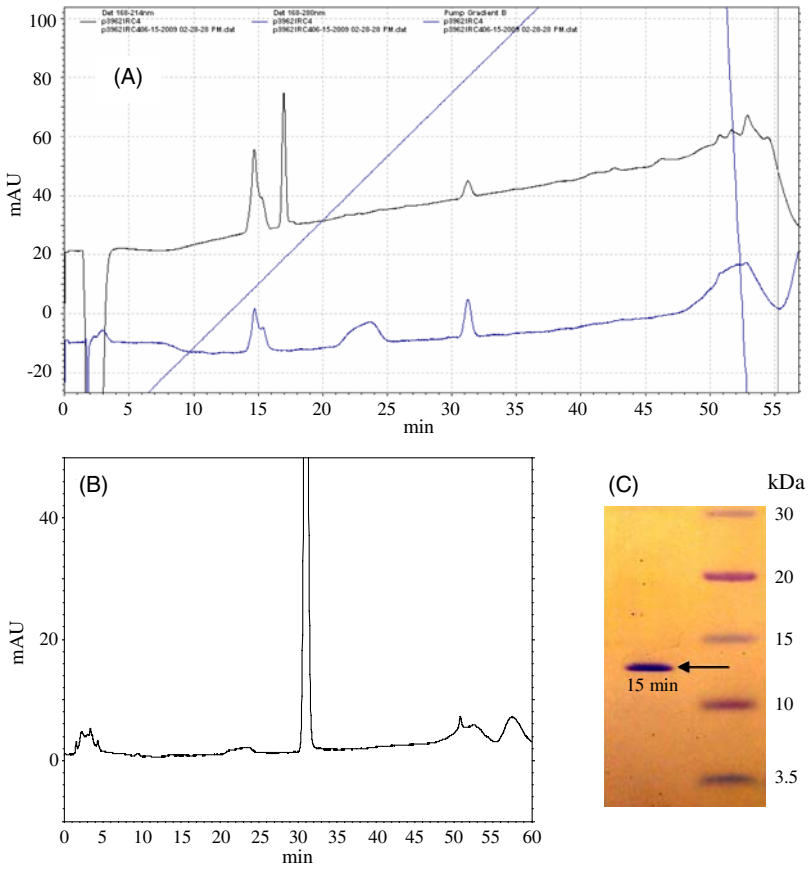


**Fig. S2.** (*A*) High-performance liquid chromatography (Reversed Phase HPLC, system gold 126B, Beckman, and software Karat for analysis). Absorption was measured for 2 wavelengths: 214 nm (measuring absorption of peptide bonds, *Upper Curve*) and 280 nm (for detecting aromatic amino acids residues, *Lower Curve*). Peaks detected at 214 nm but not at 280 nm are usually small peptides or molecules other than proteins. Peaks at 23 and 31 min also appear in a blank sample shown in panel (*B*). Fractions were collected every 1 min and samples were placed near a growing colony. Only the peak that eluted at 15 min contained the inhibitory factor. (*C*) SDS–PAGE gel electrophoresis of the sample eluting at 15 min shows the band at 12 kDa, marked with an arrow.

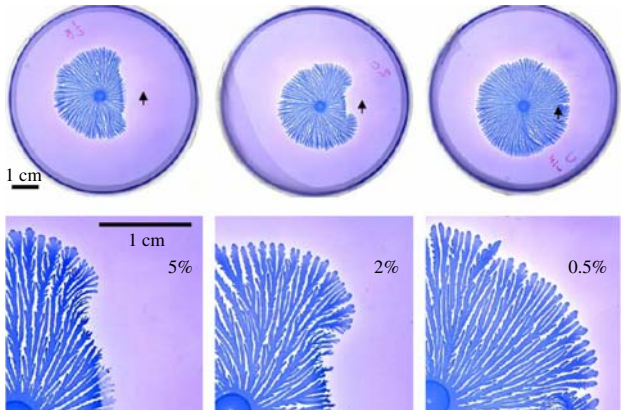


**Fig. S3.** Effect of *P. dendritiformis* Slf on colony growth. Slf at the indicated dilutions were placed near single growing colonies (1.5% agar gel with 2 g/L peptone nutrient). The lower set of images shows a higher magnification of the inhibited region shown in the upper set. Arrow indicates location of introduction of Slf, 5 μL of diluted material extracted from 20 agar plates.

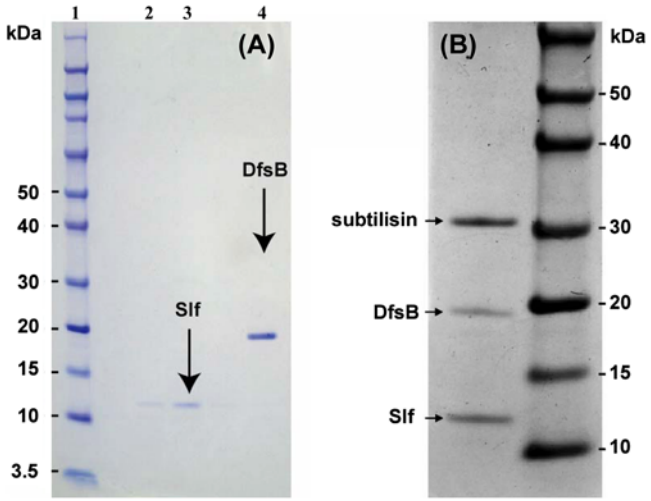


**Fig. S4.** SDS–PAGE electrophoresis of recombinant DfsB and cleavage product. (*A*) Lane 1, protein standard markers. Lanes 2 and 3, samples of the recombinant DfsB after treatment with subtilisin and HPLC purification; the treated DfsB is identified as Slf. Lane 4, DfsB isolated from *E. coli* carrying the *dfsB* expression plasmid. (*B*) Subtilisin (*Upper Band*) that was added to the 20 kDa synthesized DfsB protein (*Middle Band*) and the cleaved section Slf (*Lower Band*).

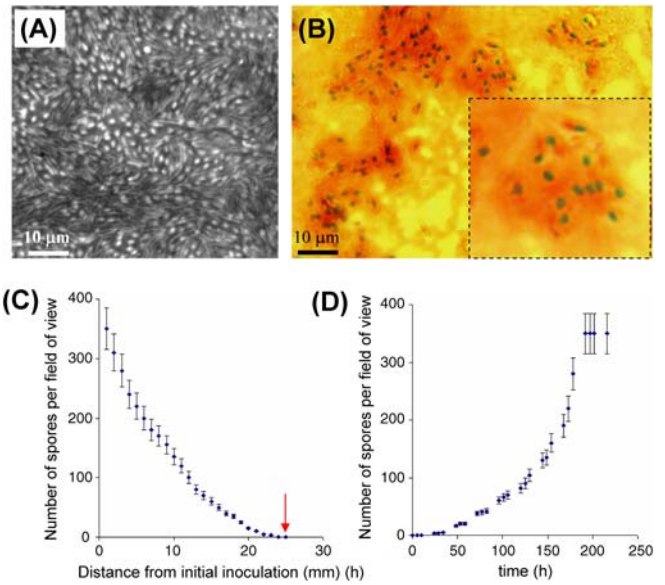


**Fig. S5.** Spores can be detected either (*A*) as white spots in an image of a living colony or (*B*) by malachite staining; here the stain is malachite green + safranine O, and the spores are the green spots, whereas the vegetative cells are pink. *P. dendritiformis* spores are smaller than *B. subtilis* spores and have a sesame seed shape (1 μm × 1.5 μm). Some appear outside the mother cell, and some appear inside the mother cell. (*C*) Distribution of spores in a colony grown for 10 d on a 1.5% agar gel containing 2 g/L peptone. Each point was determined by counting the number of visible spores in a 50 μm × 50 μm region at a given distance from the initial inoculation; an average was taken over 10 different dishes. The red arrow indicates colony's edge. (*D*) The number of spores at a fixed point (25 mm from the initial inoculation) as a function of time. The starting point $t = 0$ corresponds to the time when the colony's edge reached this location (10 d). Similarly, at any other location within a colony, the number of spores increases with time.

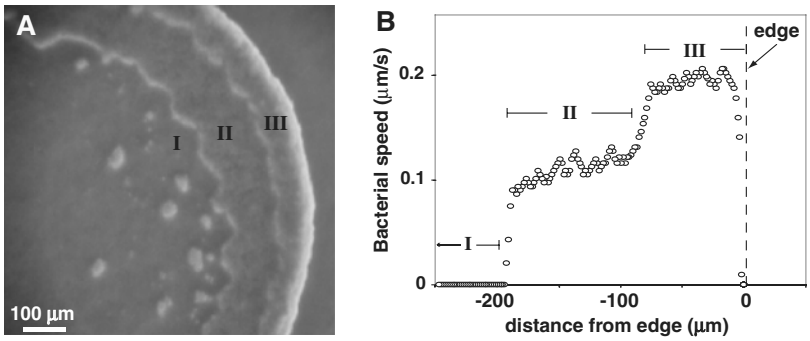


**Fig. S6.** *P. dendritiformis* bacterial colony grown on a 1.5% agar gel with 2 g/L peptone. (*A*) The image shows three well-defined regions at the colony's edge: region III, where the bacteria at the outer edge of the colony are in three layers and are very active; region II, where the bacteria are in two layers and are less active; and region I, where the bacteria are in a single layer and show little or no movement. (*B*) Average bacterial speed as a function of distance from the colony edge, which is at position 0. Bacteria in each region have a distinct fairly uniform mean speed. The mean speed is calculated by averaging the speed versus distance along many lines parallel to the horizontal direction for about 1,000 frames for five different colonies. The standard deviation of five experiments is too small to be shown. (Images taken from ref. 9) [Copyright (c) American Society for Microbiology, Journal of Bacteriology, 191, 2009, 5758-5764, 10.1128/JB.00660-09].

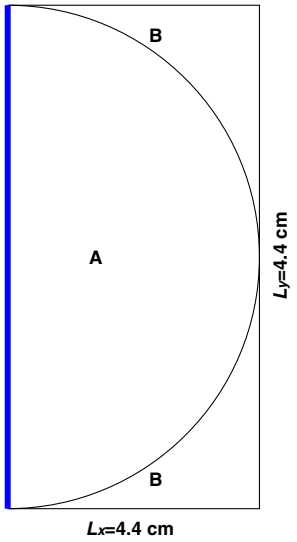


**Fig. S7.** The computational domain of the numerical simulation of two colonies. Due to symmetry, we only simulate the right colony. Also by symmetry there is no flux of the nutrients subtilisin and Slf across the left side of the rectangle (*Blue*). The boundary between regions A and B marks the edge of the Petri dish. Along this boundary there is no nutrient flux. In addition, subtilisin and Slf vanish in region B.

**Table S1. Parameters for the numerical simulation of two neighboring colonies**

| | |
|---|---|
| physical size | $L_x = 4.4$, $L_y = 8.8$ |
| diffusions | $D_b = 0.01$, $D_n = 0.01$, $D_s = 0.2$, $D_x = 0.2$ |
| bacteria | $b_{\max} = 3$ |
| | $\mu_0 = 2$, $\mu_s = 2.5$ |
| | $k_c = 20$, $k_{c0} = 5$ |
| | $\mu_{ps} = 0.7$, $a_{ps} = 0.4$, $\mu_x = 12$, $x_c = 0.02$ |
| prespores | $\mu_{sp} = 0.3$, $\mu_{px} = 12$ |
| nutrient | $\lambda_b = 0.17$, $\lambda_p = 0.15$ |
| subtilisin | $\nu_{sp} = 0.8$, $\nu_{ss} = 0.5$ |
| Slf | $\nu_x = 25$ |
| | $\nu_{xx} = 0$, $\nu_{dx} = 0.0005$, $\nu_{db} = 0.02$ |
| | $s_c = 0.55$, $b_c = 2.9$ |
| envelope | $v_{\max} = 0.15$, $a_f = 0.2$ |
| grid | $N_x = 300$, $N_y = 600$ |
| | $\Delta t = 0.2(\max\{L_x/N_x, L_y/N_y\})^2$ |
| | $K = 2$ |

The physical dimensions $L_x$ and $L_y$ correspond to the Petri dishes used in the experiments. The diffusion parameters, the maximal front speed, sporulation rate, $\mu_{sp}$, and nutrient consumption rate, $\lambda_b$, are of the order observed in experiments. Chemotaxis parameters, $k_N$ and $k_{N0}$, were chosen to give a tight profile for the bacteria near the interface. The maximal concentration of bacteria, $b_{\max}$, and subtilisin production rate, $\nu_{sp}$, are arbitrary and serve as reference to other parameters. The critical thresholds for Slf production $s_c$ and $b_c$ were chosen to be between the bacteria and subtilisin steady state values inside the colony and at the edge of a colony growing toward its neighbor. Degradation rates for subtilisin and Slf are small, as observed in experiments. All other parameters were chosen to yield a growth pattern that resembles experiments.

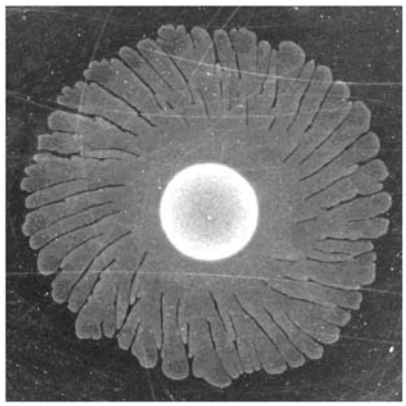

**Movie S1.** A single *P. dendritiformis* bacterial colony growing on a 1.5% agar gel with 2 g/L peptone nutrient. A droplet of Slf was introduced on the right side of the growing colony (15 mm from the colony's center, out of the frame). The growth period shown in the movie starts immediately after Slf was introduced, which was 65 h after inoculation. Frame separation is 1 h. The diameter of the initial inoculation disc is 4.5 mm. Note that the colony's branches on the right hand side vanish as time evolves.

Movie S1 (AVI)